Range Policy of Adaptive Cruise Control Vehicles for Improved Flow Stability and String Stability

Jing Zhou and Huei Peng

***Abstract*—A methodology to design the range policy of adaptive cruise control vehicles and its companion servoloop control algorithm is presented in this paper. A nonlinear range policy for improved traffic flow stability and string stability is proposed and its performance is compared against the constant time headway policy, the range policy employed by human drivers, and the Greenshields policy. The proposed range policy is obtained through an optimization procedure with traffic flow and stability constraints. A complementary controller is then designed based on the sliding mode technique. Microscopic simulation results show that stable traffic flow is achieved by the proposed method up to a significantly higher traffic density.**

***Index Terms*—Adaptive cruise control, range policy, string stability, traffic flow stability.**

I. Introduction

ADAPTIVE CRUISE CONTROL (ACC) is a driver assistance system designed to provide improved convenience and comfort. An ACC-equipped vehicle detects the presence of a preceding vehicle and measures the distance (range) as well as the relative speed (range rate) by using a forward-looking sensor. It automatically adjusts the vehicle speed to keep a proper range when a preceding vehicle is detected. When no preceding vehicle is detected, it functions like a conventional cruise control vehicle. ACC systems can be categorized into two types: "autonomous" and "nonautonomous". For an autonomous ACC, the vehicle is controlled based on self-gathered information, whereas communications with adjacent vehicles or transportation infrastructure are required for a nonautonomous system. This study is restricted to the autonomous type, which has a better chance of adoption in the near future.

Recently, ACC became available as an option on high-end passenger vehicles. It was designed mainly for increased convenience and driving comfort. However, from the transportation planners' viewpoint, ACC vehicles are likely to impact traffic characteristics, including highway safety, efficiency, and capacity because of their more consistent (and different) behavior compared with human drivers [1]. Before ACC vehicles are deployed on a large scale, their string behavior and flow characteristics need to be carefully investigated. Otherwise traffic congestion may become worse instead of being better. Whereas early ACC systems are designed mainly for applications with relatively homogeneous traffic behavior, stop-and-go cruise control systems were recently introduced to reduce driver workload under congested driving conditions, including dense urban traffic [2]. In those applications, vehicle speed is low and frequent gearshifts result in widely varied traction behavior.

Two of the most important macroscopic behaviors of ACC vehicles are traffic flow stability and string stability. Traffic flow stability [3] defines the evolution of traffic density and average velocity in response to small variation in traffic density. This characteristic is important for areas upstream of the point where traffic density disturbance is introduced, e.g., an entrance or exit ramp. A traffic flow is said to be stable (or unstable) when the traffic flow Q goes up (or down) as the traffic density ρ is increased. On the fundamental diagram, the slope $\partial Q/\partial \rho$ indicates the stability of the traffic flow [4]. When the flow–density curve demonstrates a positive slope (when the density is below the characteristic density), small density disturbance propagates as a forward traveling wave and the traffic is stable. Beyond the characteristic density (with a corresponding characteristic speed), the traffic flow becomes unstable. When the traffic flow is unstable, a small density disturbance will affect sections upstream of the disturbance source and less flow can go through. The reduced flow causes local density to go up, which further reduces flow, and eventually could result in a complete jam. When ACC systems are designed, it is desirable to adjust their headway policy so that traffic flow stability is improved. This can be achieved by ensuring that the slope $\partial Q/\partial \rho$ remains positive up to a higher traffic density (i.e., achieves a higher characteristic density). This obviously needs to be done without compromising safety.

The string stability problem of a vehicle platoon has been studied since the late 1970s [5], [6]. The term "string stability" refers to the nonamplifying upstream propagation of vehicle speed perturbation through a string of vehicles. This property ensures that the variation of preceding vehicle speed will not result in amplified fluctuations in the following vehicle speed. Equivalently, this property guarantees that any perturbation in range error that does not result in a crash downstream will not result in a crash upstream either. A common approach to study string stability is to examine the transfer function from the range error of the preceding vehicle to that of the following vehicle. If this transfer function has a magnitude of less than 1 at all frequencies, string stability is guaranteed [7].

Manuscript received March 9, 2004; revised June 28, 2004 and July 26, 2004. This work was supported in part by the Automotive Research Center at the University of Michigan. The Associate Editor for this paper was T. Dingus.

The authors are with the Department of Mechanical Engineering, University of Michigan, Ann Arbor, MI 48109-2133, USA (e-mail: hpeng@umich.edu).

Digital Object Identifier 10.1109/TITS.2005.848359

Both traffic flow stability and string stability are important macroscopic properties that are influenced by the vehicle range policy. In addition, string stability is dependent on the servoloop control algorithm. Determining a proper range policy is thus an important first step, which then needs to be complemented by a proper design of the servo control algorithm.

II. Requirements on Range Policy

Range policy [8]–[10] refers to the selection of the desired following distance as a function of vehicle operating parameters, especially the vehicle forward speed. In general, there are two types of range policies: constant range and variable range policies. For a constant range policy, the separating distance is independent of the speed of the controlled vehicle and its implementation requires intervehicular communication to ensure string stability [11]. This range policy is used primarily in automated highway research when higher flow rate is of utmost importance. As of today, no ACC system on the market uses constant range policy. In this paper, our discussion will be limited to variable range policies because requiring vehicle-to-vehicle communication is not an attractive path for ACC implementation in the immediate future.

An ACC range policy should be designed to satisfy the following attributes.

1) It should lead to increased traffic capacity and a stable traffic flow up to a higher characteristic density.
2) The selected range policy should have a companion ACC servo controller that ensures string stability without communicating with neighboring vehicles or the infrastructure.
3) It should stay close to the human drivers' range behavior, at least during the early implementation stage.
4) The control effort should be within the vehicle's traction/braking capability.
5) The range policy should not be too "sensitive." In other words, a small change in range measurement (due to sensor noise or a vehicle cut-in) should not result in a significant change in the desired vehicle speed. This attribute is related to 4), and both of them ensure that the vehicle capability is not frequently exhausted.

The overall ACC design is divided into two steps: 1) specify a range policy; and 2) design a controller for the servoloop. In this paper, the overall ACC system is assumed to have a dual-loop structure (Fig. 1). A main loop ACC controller determines the proper acceleration based on measured range, range rate, speed, and acceleration signals. A subloop controller then manipulates the engine and brake actuators to achieve the desired acceleration or deceleration. Since the emphasis of this study is on the range policy and outer loop controller, the servoloop is ignored. We assume that its behavior is approximated by a first-order system

$$\tau \dot{a}_i + a_i = a_{i,\mathrm{des}} \tag{1}$$

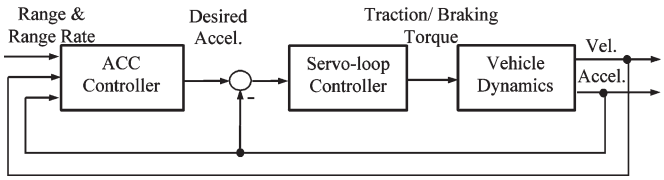

Fig. 1. Dual-loop structure of an ACC system.

where a_i is the vehicle's actual acceleration, $a_{i,\mathrm{des}}$ is the acceleration command, and τ is the servoloop time constant. The vehicle speed and position are obtained through integration.

III. Constant Time Headway Policy

The constant time headway (CTH) policy is commonly suggested as a safe practice for human drivers and is frequently used in ACC designs. The desired intervehicular range given by a CTH policy is $R_{\mathrm{des}} = A + T_{\mathrm{h}} v_i$, where A is the separation distance when the vehicle is at standstill, T_{h} is the time headway, and v_i is the host vehicle speed. Prototype ACC vehicles commonly offer a selectable time headway between 1 and 2 s. For CTH policy, a sliding mode controller without using acceleration information can be designed to guarantee string stability [9], [12]. Let e_i denote the range error, i.e., the difference between the actual range and the desired range. Define a sliding surface $S_1 \equiv e_i = R_i - T_{\mathrm{h}} v_i$, an asymptotically converging algorithm can be obtained by imposing the requirement

$$\dot{S}_1 = \dot{e}_i = -\lambda S_1 \tag{2}$$

where λ is the convergence rate of the sliding surface. Since $\dot{R}_i = v_{i-1} - v_i$, the desired acceleration is

$$a_{i,\mathrm{des}} = \frac{\lambda}{T_{\mathrm{h}}} e_i + \frac{1}{T_{\mathrm{h}}} \dot{R}_i. \tag{3}$$

It can be seen that $a_{i,\mathrm{des}}$ is inversely proportional to T_{h}, i.e., short time headway necessitates aggressive control effort and is at higher risk of losing string stability. To avoid string instability, a necessary lower bound on T_{h} is $T_{\mathrm{h}} \geq 2\tau$ [13], where τ is the time constant of the servoloop [see (1)]. Typically, τ varies between 0.5 and 1.0 s and is dependent on the vehicle speed and power-to-weight ratio. When the vehicle servoloop response is slow, the ACC time headway needs to be large to maintain string stability. The fact that practicable T_{h} is dependent on τ signifies the importance of the main loop control design.

One deficiency of controller (3) is that it is unaware of the existence of servoloop dynamics. To relax the time headway limit ($T_{\mathrm{h}} \geq 2\tau$), a more robust control algorithm needs to be designed. If host vehicle acceleration is available for feedback, an augmented sliding mode controller can be synthesized [12]

$$a_{i,\mathrm{des}} = \left(1 - \frac{\tau T_{\mathrm{h}}}{T_a}\right) a_i + \frac{\tau}{T_a} \dot{R}_i + \frac{\tau \lambda}{T_a} \varepsilon_i. \tag{4}$$

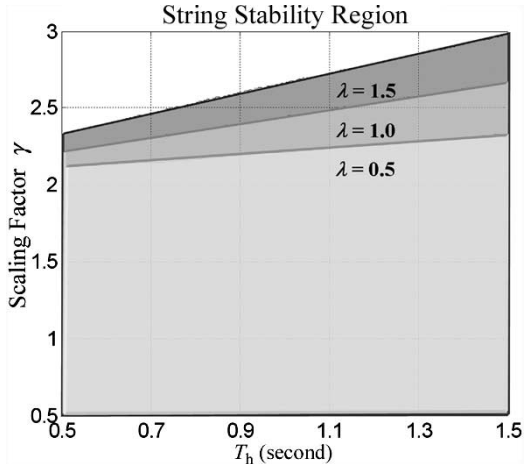

Fig. 2. The influence of time constant uncertainty on string stability for the controller in (5).

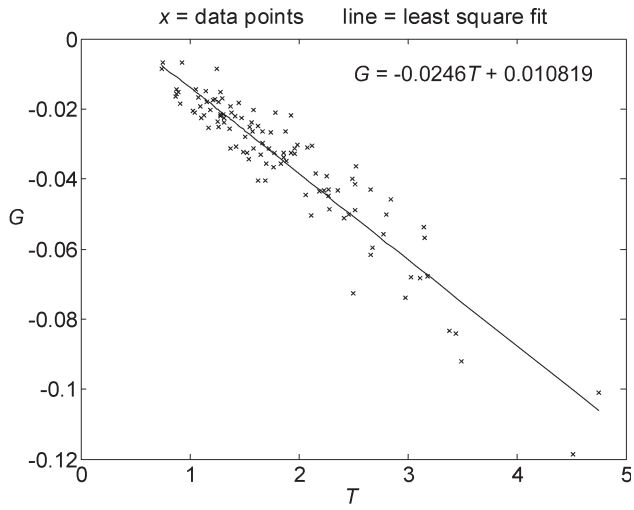

Fig. 3. Relationship between coefficients T and G.

For this controller, a compound range error is used $\varepsilon_i = R_i - T_\mathrm{h} v_i - T_a a_i$, where $T_a > 0$ is a control gain to be selected. It can be shown that if the time constant τ is perfectly known, the string stability condition is guaranteed if $T_\mathrm{h}^2 \geq 2T_a > 0$. Consequently, by defining a special range error and incorporating the servoloop time constant explicitly into the controller, we eliminate the dependence of T_h on τ. In practice the servoloop is not exactly a first-order system, or its time constant τ is not perfectly known. Consequently, the controller is reformulated as

$$a_{i,\mathrm{des}} = \left(1 - \frac{\tau_\mathrm{e} T_\mathrm{h}}{T_a}\right) a_i + \frac{\tau_\mathrm{e}}{T_a}\dot{R}_i + \frac{\tau_\mathrm{e}\lambda}{T_a}\varepsilon_i \tag{5}$$

where τ_e is the estimated time constant. The relationship between the actual and estimated time constant is assumed to be $\tau = \gamma\tau_\mathrm{e}$, where γ is an uncertainty scaling factor. Fig. 2 indicates that the controller in (5) is not sensitive to the uncertainty in τ. For a slow convergence rate ($\lambda = 0.5$), string stability can be maintained even when the actual time constant is twice as long as the estimated value τ_e.

The influence of range policy on traffic flow can be demonstrated on the fundamental diagram, which depicts the relationship between traffic flow rate and traffic density. By assuming a uniform vehicle length $L = 5$ m, the traffic density at steady state is given by $\rho = 1/(L + A + T_\mathrm{h} v)$. When the flow is constrained, i.e., when vehicles cannot drive at their free flow speeds, the flow rate is $Q = \rho v = 1/T_\mathrm{h} - (L + A)\rho/T_\mathrm{h}$. Since the separation distance A must be positive (else collision occurs at low speeds), the slope $\mathrm{d}Q/\mathrm{d}\rho$ is negative. Therefore the traffic flow is always unstable whenever the traffic density is in the constrained flow section.

In summary, although the CTH policy is easy to implement and a servo controller can be readily designed to ensure string stability, it has poor traffic flow stability in the constrained flow region. In other words, it is prone to unstable flow under density disturbance. For this reason, we believe that the CTH range policy is not the best range policy one can use.

IV. Range Policy Used by Human Drivers

Even though driver behavior varies widely, human driving data can be used to identify an averaged human range policy. One such averaged driver behavior was recently extracted from the University of Michigan Transportation Research Institute's (UMTRI) Intelligent Cruise Control Field Operational Test (ICCFOT) database [14]. In this study, driving behaviors of 107 drivers were recorded. Near steady state data were collected and the human range behavior was identified. The human range policy was found to be in the form of a quadratic curve

$$R = A + Tv + Gv^2 \tag{6}$$

where A is the clearance at standstill and T and G are the coefficients identified by curve fitting. The parameter T for individual drivers turned out to fall mostly between 1 and 2.5 s. The parameter G was found to be strongly correlated to T by the relation $G = -0.0246T + 0.0108$ (Fig. 3). Interestingly, all 107 human drivers in the ICCFOT database exhibit a negative value of G, i.e., at higher vehicle speeds the effective time headway ($\mathrm{d}R/\mathrm{d}v$) reduces.

Another curve fitting result of human driver behavior was reported in [15]. It takes the form of a power function $R = 2 + 6.33v^{0.48}$. The comparison of these two observed human driver range policies is presented in Fig. 4. Despite notable mismatch in the specific range values, they are similar qualitatively. In addition, both models indicate that human drivers tend to adopt a smaller effective time headway at higher vehicle speed.

The traffic flow characteristics of the quadratic range policy are analyzed below. At steady state, the traffic density is $\rho = 1/(L + A + Tv + Gv^2)$. Flow rate can then be formulated as a function of ρ

$$Q = \rho v = \rho \frac{\sqrt{T^2 - 4G\left(L + A - \frac{1}{\rho}\right)} - T}{2G}. \tag{7}$$

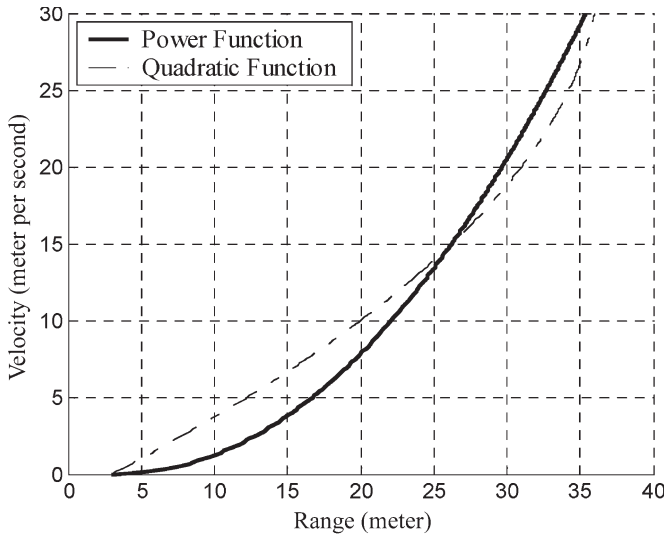

Fig. 4. Range policies employed by human drivers.

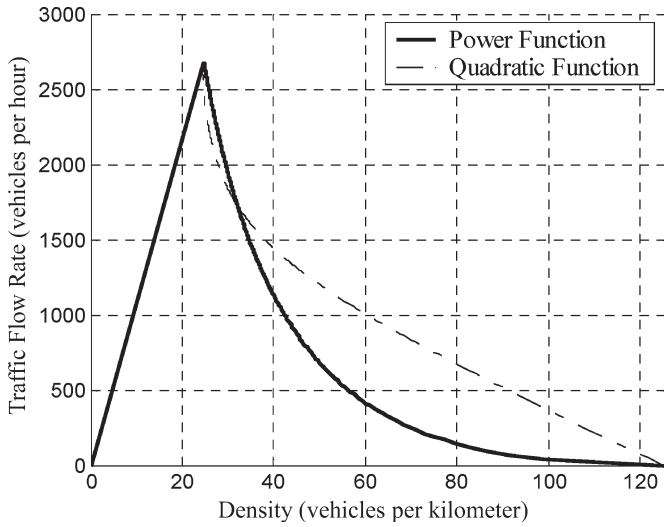

Fig. 5. Fundamental diagram of human range policies.

Take the derivative and set it to zero $\mathrm{d}Q/\mathrm{d}\rho = 0 \Rightarrow$

$$\sqrt{T^2 - 4G\left(L + A - \frac{1}{\rho}\right)} - \frac{2G}{\rho\sqrt{T^2 - 4G\left(L + A - \frac{1}{\rho}\right)}} - T = 0. \quad (8)$$

Solve (8) and accept only the positive solution

$$\rho_{\mathrm{cr}} = \frac{1}{2(L + A) + T\sqrt{\frac{(L+A)}{G}}}. \quad (9)$$

The critical density ρ_{cr} is the density when maximum traffic flow is obtained, which also marks the boundary between stable and unstable traffic flow. A solution for (9) exists only when G is positive, and traffic capacity can be obtained by substituting ρ_{cr} into (7) as long as ρ_{cr} exists. When G is negative, the slope $\mathrm{d}Q/\mathrm{d}\rho$ is always negative in the constrained flow section.

The fundamental diagrams of the above two nonlinear range policies are shown in Fig. 5. The maximum flows of these two policies are achieved when the vehicles are at the boundary between free flow and constrained conditions. When the flow becomes constrained, traffic volume starts to decrease with increased density. Like the CTH policy, the traffic flow is always unstable in the constrained region due to the negative definiteness of $\mathrm{d}Q/\mathrm{d}\rho$. For human drivers, G is always negative (Fig. 3), which indicates that vehicle strings formed by human drivers are "more unstable" than ACC vehicles using the CTH range policy. In other words, if we design ACC range policies to be close to the human driver's natural behavior, the resulting traffic flow stability will be even worse than vehicles using the CTH range policy. Requirement 3 (humanlike) listed in Section II is thus a conflicting goal with requirement 1 (more stable traffic flow).

V. Synthesis of a Range Policy for Traffic Flow Stability and String Stability

The goal of this section is to devise a range policy to achieve a stable traffic flow up to a higher critical density than both human and CTH range policies. The following facts can be derived from (9): 1) the quadratic range policy has a local maximum in the constrained flow section on the fundamental diagram only if G is positive; 2) if A, T, and G are all positive, the critical density is upper bounded $\rho_{\mathrm{cr}} < [1/2(L + A)] = (1/2)\rho_{\mathrm{jam}}$.

The proposed range policy will be built based on these two facts. A quadratic policy with structure similar to (6) is used. For traffic flow stability, G is chosen to be positive and A is fixed at 3 m (the uniform separating distance at standstill). Because the acceleration command is inversely proportional to time headway, the slope $\mathrm{d}R/\mathrm{d}v$ should be lower bounded for the sake of string stability. In addition, to characterize control effort quantitatively, the sensitivity [10] of a range policy is defined as $S = (1/2)(\mathrm{d}v_{\mathrm{des}}^2/\mathrm{d}R) = v_{\mathrm{des}}(\mathrm{d}v_{\mathrm{des}}/\mathrm{d}R)$. It has a unit the same as the acceleration and represents how much kinetic energy per unit mass should be accumulated or dissipated in response to a unit change of the desired range. A higher sensitivity value indicates a higher demand on the vehicles' acceleration and braking capabilities. The range policy selection is formulated as a constrained optimization problem as follows.

1) Objective: Design T and G to maximize the traffic capacity.
2) Subject to the constraints:
   a) The range should be a nondecreasing function of the forward speed, i.e., $\mathrm{d}R/\mathrm{d}v \geq 0$.
   b) $G > 0$ for stable traffic flow.
   c) Critical density ρ_{cr} should be maintained close to its upper limit $1/[2(L + A)]$. A constraint $\rho_{\mathrm{cr}} \geq 0.0624$ (vehicles/m) is imposed.

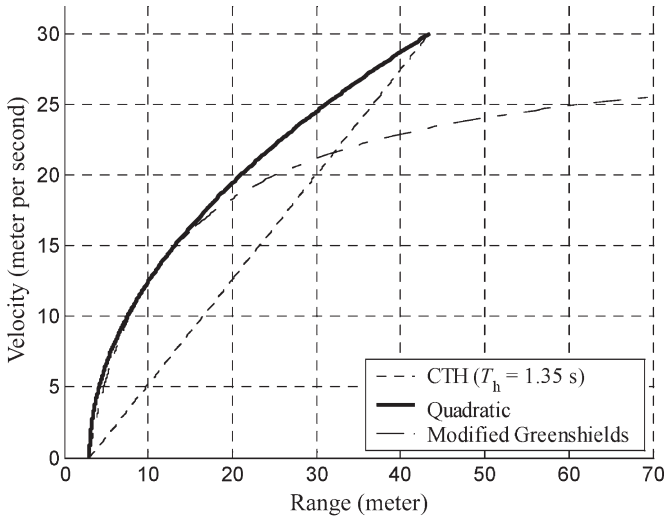

Fig. 6. The proposed quadratic range policy; also presented are a CTH policy and the Greenshields policy.

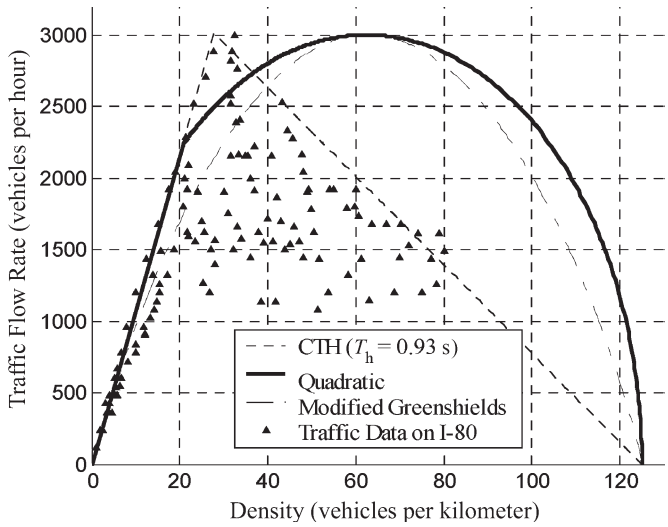

Fig. 7. The traffic flow characteristics of a CTH policy, the proposed quadratic policy, the modified Greenshields, and the measured highway data.

d) The maximum sensitivity over the entire speed range is limited to 12 $\mathrm{m/s^2}$.
e) The slope $\mathrm{d}R/\mathrm{d}v$ at 5 m/s must be higher than 0.45 s (for string stability).

This optimization problem is converted into the negative null form and solved by using the Matlab Optimization Toolbox. Given the specification $\rho_{\mathrm{cr}} = 62.4$ vehicles/km, the range law is obtained $R = 3 + 0.0019v + 0.0448v^2$, with critical velocity $v_{\mathrm{cr}} = 13.4$ m/s. This nonlinear range policy is illustrated in Fig. 6 together with a CTH policy and a modified Greenshields policy for comparison.

In 1935, Greenshields [16] derived a parabolic equation for the flow–density relationship on the basis of a linear velocity–density assumption

$$v = V_{\mathrm{f}}\left(1 - \frac{\rho}{\rho_{\mathrm{jam}}}\right) \tag{10}$$

$$Q = \rho V_{\mathrm{f}}\left(1 - \frac{\rho}{\rho_{\mathrm{jam}}}\right) \tag{11}$$

where V_{f} is the free-flow speed and ρ_{jam} is the jam density. Greenshields' model and its derivatives dominated the field for nearly 50 a and were accepted for their agreement with measured human driving data. In [10], a modified Greenshields range policy was employed in the ACC system to demonstrate its superiority over CTH policy in terms of traffic flow stability

$$v = V_{\mathrm{f}}\left[1 - \left(\frac{\rho}{\rho_{\mathrm{jam}}}\right)^{l}\right]^{m} \tag{12}$$

$$Q = \rho V_{\mathrm{f}}\left[1 - \left(\frac{\rho}{\rho_{\mathrm{jam}}}\right)^{l}\right]^{m} \tag{13}$$

where l and m can be manipulated to meet particular specifications on traffic capacity and critical density. This modified Greenshields policy leads to a stable flow up to the critical density $\rho_{\mathrm{cr}} = \rho_{\mathrm{jam}}[1/(1+lm)]^{1/l}$. At ρ_{cr} the corresponding speed is $v_{\mathrm{cr}} = V_{\mathrm{f}}[lm/(1+lm)]^{m}$, based on which traffic capacity can be obtained. A typical plot of the modified Greenshields range policy is also shown in Fig. 6. This range policy has a notable problem: its range at high speeds is unreasonably large, which may invite frequent cut-ins and practically discourage the driver from using it.

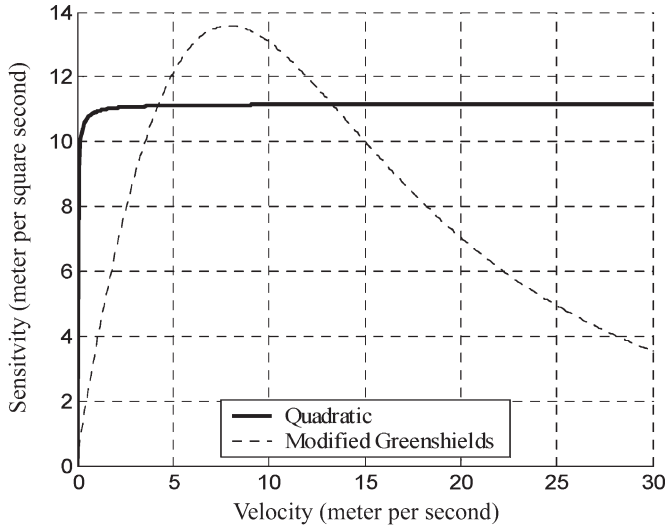

Fig. 8. Sensitivities of the proposed quadratic range policy and the Greenshields policy.

Fig. 7 presents the traffic flow characteristics of three range policies. The points shown in triangle symbols are $Q - \rho$ data under various conditions measured from a single lane on a multiple-lane highway [17]. They represent actual traffic characteristics of human drivers. The three range policies are chosen to yield the same traffic capacity of about 3000 vehicles/h to make the comparison fair. The critical densities of the suggested quadratic range policy and Greenshields policy are considerably higher than that of the CTH policy (62.4 vs.

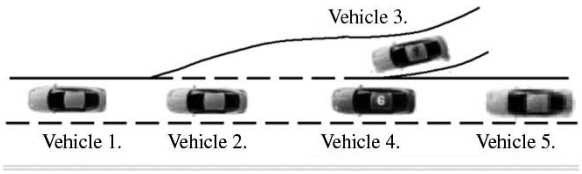

Fig. 9. Merging simulation scenario.

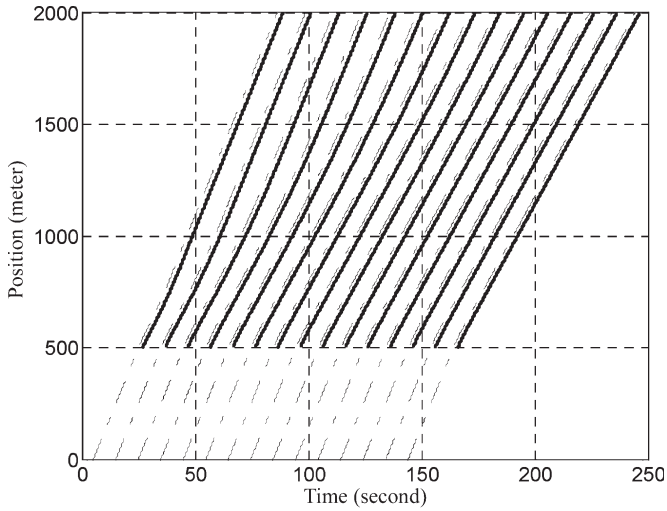

Fig. 10. Space–time chart of the ACC vehicles.

27.8 vehicles/km), thus their traffic flow stability regions are significantly extended. Over the entire traffic density range, the proposed quadratic range policy yields higher traffic volume than the Greenshields.

Although the traffic flow of the proposed range policy is higher than that of the Greenshields policy, Fig. 8 shows the maximal sensitivity of the proposed policy is lower than that of the Greenshields (11.2 vs. 13.6 $\mathrm{m/s^2}$). The proposed quadratic range policy has a near-constant sensitivity over a wide speed range (Fig. 8), whereas the Greenshields has a peak at the medium speed range. In summary due to its simple form, increased critical density, higher traffic volume, and lower sensitivity, the proposed quadratic policy does seem to be a viable alternative compared with the CTH or the Greenshields policy.

VI. Controller for Nonlinear Range Policy

A sliding mode control algorithm is designed to implement the nonlinear range policy proposed in the previous section. To begin with we define a compound range error for the new range policy

$$\varepsilon_i = R_i - \left(A + Tv_i + Gv_i^2\right) - T_a a_i \tag{14}$$

where T_a is a positive parameter to be determined. The sliding surface is selected to be $S_2 = \varepsilon_i$. To ensure sliding motion, the relationship $\dot{S}_2 = \dot{\varepsilon}_i = -\lambda S_2$ is imposed. Substitute the simplified subloop dynamics (1) into the sliding motion condition

$$\dot{R}_i - T_v a_i - T_a \frac{(a_{i,\mathrm{des}} - a_i)}{\tau} = -\lambda \varepsilon_i \tag{15}$$

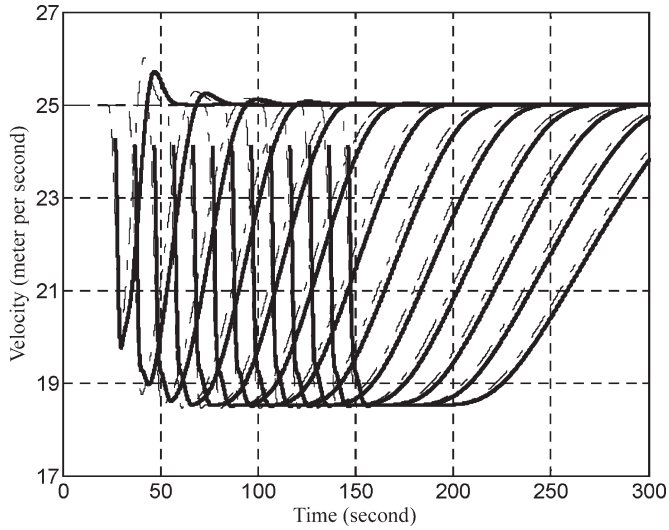

Fig. 11. Speed of ACC vehicles in the merging simulation.

where the equivalent time headway $T_v \equiv \mathrm{d}R/\mathrm{d}v = T + 2Gv_i$. As a result the acceleration command is

$$a_{i,\mathrm{des}} = \left(1 - \frac{\tau T_v}{T_a}\right) a_i + \frac{\tau}{T_a}\dot{R}_i + \frac{\tau\lambda}{T_a}\varepsilon_i. \tag{16}$$

The sliding mode control guarantees stability for individual vehicles, namely range error and velocity error will converge to zero asymptotically. In order to investigate its string stability characteristics, the ACC system is linearized around a nominal vehicle speed $v_{0,i} = v_{0,i+1} = v_0$ and the corresponding range $R_{0,i} = R_{0,i+1} = R_0$ with $R_0 = A + Tv_0 + Gv_0^2$. At a certain moment, the lead vehicle speed is perturbed, thus introducing disturbance to the trailing vehicles. Let $v_i = v_0 + \Delta v_i$, $\dot{v}_i = \Delta\dot{v}_i$, and $R_i = R_0 + \Delta R_i$, $\dot{R}_i = \Delta\dot{R}_i$. It can be shown [13] that for linearized systems the transfer function of the range error propagation is the same as that of the speed variation

$$G(s) = \frac{e_i(s)}{e_{i-1}(s)} = \frac{\Delta v_i(s)}{\Delta v_{i-1}(s)}. \tag{17}$$

Therefore, the study on string stability boils down to checking the maximum magnitude of the transfer function of the velocity variation. We choose T_a to be $T_a = T_v^2/k = (T + 2Gv_i)^2/k$, where k is a scaling factor. Under the assumption that deviations from the nominal range and vehicle velocity are small, combine (1) and (16), the transfer function of speed variation is

$$\frac{\Delta v_i}{\Delta v_{i-1}}(s) = \frac{k\tau s + k\tau\lambda}{\tau T_v^2 s^3 + (k\tau T_v s^2 + \tau\lambda T_v^2 s^2) + (k\tau s + k\tau\lambda T_v s) + k\tau\lambda}. \tag{18}$$

To ensure string stability, the magnitude inequality $\|\Delta v_i(s)/\Delta v_i(s)\| \le 1$ must hold for all frequencies, therefore the requirement is reduced to

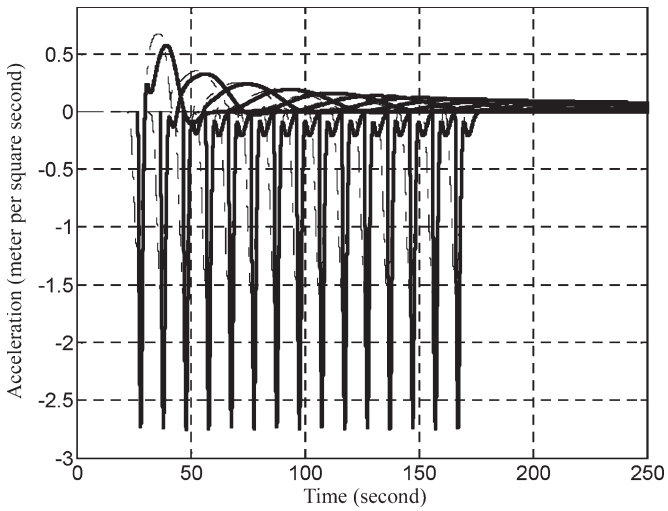

Fig. 12. Acceleration of ACC vehicles in the merging simulation.

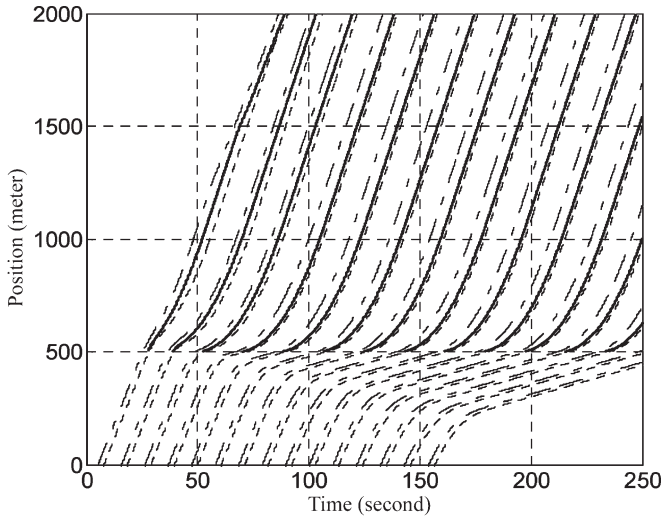

Fig. 13. Space–time chart for ACC vehicles with CTH range policy.

$$T_v^2\omega^4 + \left(k^2 - 2k + \lambda^2 T_v^2\right)\omega^2 + (k^2 - 2k)\lambda^2 \geq 0. \qquad (19)$$

After some algebraic reductions, it is found that this inequality constraint is always satisfied if $k > 2$. The control law in (16) together with the condition $k > 2$ guarantees that the desired nonlinear range policy is tracked in a string-stable fashion provided that the speed variation is so small that the linear assumption still holds.

VII. Simulation Results

The effectiveness of the nonlinear controller to maintain the proposed range policy will be verified by simulations. The scenario is as follows (Fig. 9): the vehicles on the main lane are confined to travel in a single lane of the highway. An on-ramp is located 500 m downstream from the highway entrance. When the average position of vehicles 2 and 4 crosses the end of the ramp, vehicle 3 merges into the main lane, i.e., almost right in the middle between vehicles 2 and 4. The speed of vehicle 3 is assumed to match that of vehicle 2; however, its initial range may deviate from its desired value. At this very moment the lead vehicle of vehicle 4 switches from vehicle 2 to vehicle 3. Although only five vehicles are shown in Fig. 9, this merging process is repeated for every four vehicles entering the main lane. In the following simulation, the cruising speed on the highway is 25 m/s, which is higher than the critical velocity $v_{\rm cr}$ (13.4 m/s), so we should expect to observe stable traffic flow. All of the vehicles are assumed to adopt the nonlinear range policy proposed in Section V and are equipped with the ACC controller in (16). It is assumed that all vehicles have a subloop time constant $\tau = 0.8$ s [see (1)], but in the ACC controllers its estimated value is $\tau_{\rm e} = 1.0$ s. To ensure that the acceleration and deceleration efforts are within practical range, we limit the acceleration within $a_{\max} = 0.7664$ and $a_{\min} = -3.5388(\mathrm{m/s^2})$, which are extracted from human driving data [18].

Figs. 10–12 show the position, velocity, and acceleration histories of selected vehicles during the merging process. The simulation involves more than 150 vehicles. Instead of presenting the trajectories of all vehicles, only two out of every ten vehicles are shown here. In each plot there are two groups of curves. The thick solid lines are the trajectories of the merging vehicles and the thin dash–dotted lines represent the vehicles originally in the main lane. In a space–time chart, the speed of moving vehicles determines the slope of the trace, and stationary vehicles appear as horizontal lines. Fig. 10 indicates that although vehicles merging into the traffic continually induce density disturbance to the traffic flow on the main lane, the traffic density recovers its original value downstream and the traffic flow remains stable as anticipated. In Fig. 11, the abrupt drop of speed is caused by the sudden change of measured range. However, it is apparent that the velocities are lower bounded and no vehicle comes to a stop and the traffic will not accumulate near the ramp intersection. Fig. 12 shows that the string stability is maintained, since the peak values of the acceleration attenuate upstream, both acceleration and deceleration will not exceed the vehicle's capability.

Fig. 13 shows the behavior of vehicles using the CTH policy. The main loop controller takes the form of (5), which is a linear counterpart for (16). The result indicates that traffic builds up upstream of the ramp intersection, so the flow is unstable given the density disturbance input, which is in agreement with the analysis results.

For comparison purposes, a modified Gipps model is used to predict how humans will react in the same merging maneuver. The modified Gipps model is based on the original Gipps model [19], [20], but is modified to match the ICCFOT measurement data [18]. The model assumed that the driver wants to travel as fast as possible, at the same time subject to safety concern and vehicle performance limits. The vehicle speed of the modified Gipps model is given by (20) shown at the top of the next page.

The definition and values of the model parameters are explained in Table I. The values are the average of 107 human drivers identified in [18]. Fig. 14 shows that some curves have near-zero slopes after 150 s, which means those vehicles stop

$$v_n(t+\tau_r) = \min \begin{cases} v_n(t) + 2.5a_n\tau_r\left(1 - \frac{v_n(t)}{V_f}\right)\sqrt{0.025 + \frac{v_n(t)}{V_f}} \\ b_n\tau_r + \sqrt{(b_n\tau_r)^2 - b_n\left[2\left[x_{n-1} - x_n - R_{\min} - v_n(t)\tau_r\right] - \frac{v_{n-1}(t)^2}{\hat{b}}\right]} \end{cases}. \tag{20}$$

TABLE I
PARAMETERS IN THE MODIFIED GIPPS MODEL

Symbol	Description	Value
a_n	Peak acceleration	0.7664 m/s^2
V_f	Free-flow velocity	30 m/s
b_n	Peak deceleration	-3.5388 m/s^2
$\hat{b}$	Estimated peak deceleration of the preceding vehicle	-4.0 m/s^2
$R_{\min}$	Separating distance at standstill	3.5094 m
τ_r	Apparent reaction time	0.67 s

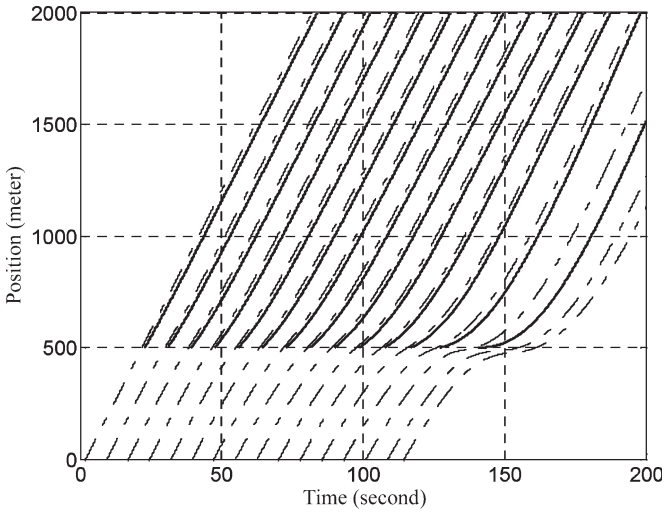

Fig. 14. Traffic space–time chart for human controlled vehicles.

completely and the traffic is accumulating near the entrance ramp. Fig. 15 confirms that vehicle speed drops to zero near the ramp intersection and both flow stability and string stability are lost.

From these simulation results, it can be seen that the proposed ACC range policy maintains traffic flow stability under challenging conditions, which is beyond the competence of human drivers. The companion control law proves to be effective in regulating the range error and preserving string stability for the nonlinear range policy.

VIII. CONCLUSION

The design of an ACC range policy and a companion control policy is presented in this paper. The proposed range policy is obtained from a constrained optimization procedure, which balances between flow stability, string stability, and sensitivity. One of the imposed constraints extends the traffic flow stability region to much above what was observed in manual driving.

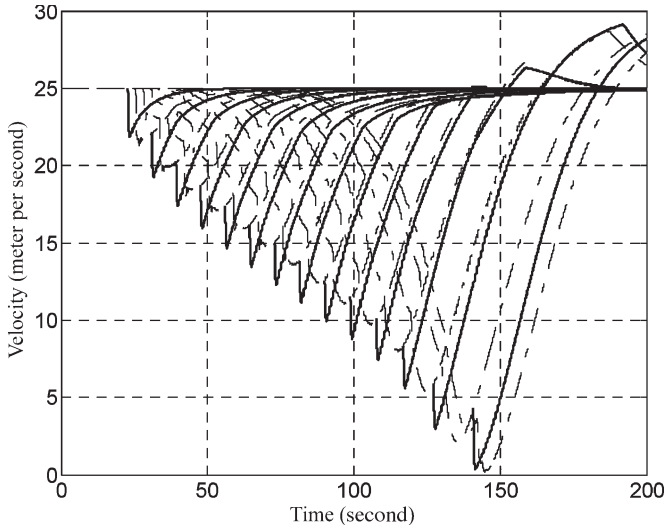

Fig. 15. Vehicle speed with human drivers in the merging simulation.

The behavior of the proposed algorithm is compared with human drivers as well as a modified Greenshields policy. It is confirmed that higher critical density and lower maximum sensitivity are achieved. A nonlinear ACC controller based on the sliding mode technique is designed to ensure string stability. A merging simulation is conducted to verify the analysis results.

ACKNOWLEDGMENT

The authors wish to thank P. Fancher of UMTRI for providing valuable data and insightful discussions.

REFERENCES

[1] P. Zwaneveld and B. van Arem, "Traffic effects of automated vehicle guidance systems," in *5th World Congr. Intelligent Transport Systems*, Seoul, South Korea, Oct. 1998.
[2] P. Venhovens, K. Naab and B. Adiprasito, "Stop and go cruise control," in *Proc. FISITA World Automotive Congr.*, Seoul, South Korea, Jun. 2000, pp. 61–69.
[3] D. Swaroop and K. R. Rajagopal, "Intelligent cruise control systems and traffic flow stability," *Transp. Res., Part C*, vol. 7, no. 6, pp. 329–352, 1999.
[4] M. Papageorgiou, "Application of automatic control to traffic flow problems," in *Lecture Notes in Control and Information Sciences*, vol. 50. Berlin, Germany: Springer-Verlag, 1983.
[5] R. J. Caudill and W. L. Garrard, "Vehicle-follower longitudinal control for automated transit vehicles," *ASME J. Dyn. Syst. Meas. Control*, vol. 99, no. 4, pp. 241–248, Dec. 1977.
[6] S. Shladover, "Longitudinal control of automotive vehicles in close-formation platoons," *ASME J. Dyn. Syst. Meas. Control*, vol. 113, no. 2, pp. 231–241, 1991.

[7] P. Ioannou and C. C. Chien, "Autonomous intelligent cruise control," *IEEE Trans. Veh. Technol.*, vol. 42, pp. 657–672, Nov. 1993.
[8] K. Santhanakrishnan and R. Rajamani, "On spacing policies for highway vehicle automation," in *Proc. American Control Conf.*, Chicago, IL, Jun. 2000, pp. 1509–1513.
[9] D. Swaroop, J. K. Hedrick, C. C. Chien and P. A. Ioannou, "A comparison of spacing and headway control laws for automatically controlled vehicles," *Veh. Syst. Dyn.*, vol. 23, no. 8, pp. 597–625, 1994.
[10] D. Swaroop and R. Huandra, "Intelligent cruise control system design based on a traffic flow specification," *Veh. Syst. Dyn.*, vol. 30, no. 5, pp. 319–344, 1998.
[11] S. Shladover, "An overview of the automated highway systems program," *Veh. Syst. Dyn.*, vol. 24, no. 6–7, pp. 551–595, 1995.
[12] J. Zhou and H. Peng, "String stability conditions of adaptive cruise control algorithms," in *IFAC Symp. Advances Automotive Control*, Salerno, Italy, Apr. 2004.
[13] C.-Y. Liang, "Traffic-friendly adaptive cruise control design," Ph.D. dissertation, Dept. Mech. Eng., Univ. Michigan, Ann Arbor, 2000.
[14] P. Fancher *et al.*, *Research on Desirable Adaptive Cruise Control Behavior in Traffic Streams*. Ann Arbor, MI: University of Michigan Transportation Research Institute (UMTRI), 2002. UMTRI-2002-16.
[15] Q. Xu, K. Hedrick, R. Sengupta and J. VanderWerf, "Effects of vehicle–vehicle/roadside–vehicle communication on adaptive cruise controlled highway systems," in *Proc. IEEE Vehicular Technology Conf.*, Vancouver, Canada, Sep. 2002, pp. 1249–1253.
[16] B. D. Greenshields, "A study of traffic capacity," in *Proc. Highw. Res. Board*, 1935, vol. 14, pp. 448–477.
[17] K. M. Kockelman, "Modeling traffic's flow–density relation: Accommodation of multiple flow regimes and traveler types," *Transportation*, vol. 28, no. 4, pp. 363–374, 2001.
[18] K. Lee and H. Peng, "Identification of a longitudinal human driving model for adaptive cruise control performance assessment," in *Proc. IMECE*, New Orleans, LA, 2002. IMECE2002-DSC-32089.
[19] P. G. Gipps, "A behavioral car following model for computer simulation," *Transp. Res. Board*, vol. 15B, no. 2, pp. 105–111, 1981.
[20] N. Gartner, C. J. Messer and A. K. Rathi. (1998). *Traffic flow theory—A state-of-the-art report: Revised monograph on traffic flow theory* [Online]. Available: http://www.tfhrc.gov/its/tft/tft.htm.

Jing Zhou received the B.S. and M.S. degrees in automotive engineering from Tongji University, Shanghai, China, in 2000.

He is currently taking the Ph.D. degree in mechanical engineering at the University of Michigan, Ann Arbor. His research interests are intelligent transportation systems with emphasis on adaptive cruise control systems as well as vehicle dynamics.

Huei Peng received the Ph.D. degree in mechanical engineering from the University of California, Berkeley, in 1992.

From 1995 to 1997, he served as the Chair of the American Society of Mechanical Engineers (ASME) Dynamic Systems and Control Division (DSCD) Transportation Panel. He is currently an Associate Professor at the Department of Mechanical Engineering, University of Michigan, Ann Arbor, and an Associate Editor for the IEEE/ASME TRANSACTIONS ON MECHATRONICS. His research interests include adaptive control and optimal control, with emphasis on their applications to vehicular and transportation systems.

Dr. Peng has been an active Member of the Society of Automotive Engineers and the ASME DSCD, New York. He received the National Science Foundation Career award in 1998.